

Improvements of the longitudinal magnetic field measurement at the HSOS/SMFT.

Plotnikov A.A.¹, Kutsenko A.S.¹, Yang S.², Kuzanyan K.M.³

- 1) Crimean Astrophysical Observatory (Russian Academy of Sciences), Nauchny, Crimea, Russia
- 2) National Astronomical Observatories of China (Chinese Academy of Sciences), Beijing, China
- 3) IZMIRAN, Troitsk, Moscow, Russia

The weak-field approximation implying linear relationship between Stokes V/I and longitudinal magnetic field, B_z , often suffers from the saturation observed in strong magnetic field regions such as sunspot umbra. In this work we intend improve the magnetic field observations carried out by the Solar Magnetic Field Telescope (SMFT) at the Huairou Solar Observing Station, China. We propose to use non-linear relationship between Stokes V/I and B_z to derive magnetic field. To determine the form of the relationship we perform comparison of SMFT data and magnetograms provided by the Helioseismic and Magnetic Imager onboard the Solar Dynamics Observatory. The algorithm of the magnetic field deriving is described in details. We show that using of non-linear relationship allows eliminating the magnetic field saturation inside sunspot umbra.

Introduction

The Solar Magnetic Field Telescope (SMFT) is a narrow-band filtergraph installed at the Huairou Solar Observing Station (HSOS), National Astronomical Observatories, Chinese Academy of Sciences [1]. The telescope provides uninterrupted homogeneous data on solar vector magnetic field since 1987. Such a long unique data series allow one to analyze long-term variations and cycle dependence of active region parameters that rely on the vector magnetic field measurements, for example, current helicity of active regions.

SMFT uses photospheric Fe-I 5324.18 Å spectral line to derive information on solar magnetic fields. Stokes V/I are routinely measured at a single point in the wing of the spectral line (20 mÅ from the line center). The magnetic field is obtained in the framework of the weak-field approximation implying linear relationship between the measured Stokes V/I and longitudinal magnetic field, B_{\parallel} :

$$B_{\parallel} = C_{\parallel} V/I. \quad (1)$$

The calibration coefficient C_{\parallel} for HSOS/SMFT measurements was analytically obtained for the first time by Ai [2]. Several other methods for weak-field calibration were proposed recently [3].

In fact, the linear relationship between the Stokes V/I and longitudinal magnetic field B_z holds as long as the magnetic field does not exceed approximately 1000 G. For stronger magnetic fields that are readily observed in the umbra of sunspots the Stokes V/I decreases resulting in the significant underestimation of the sunspot's magnetic field.

Measurements of the transversal magnetic field are complicated by the so-called 180-degree ambiguity when the azimuthal direction of the transversal magnetic field vector could not be

defined from the observations. A number of techniques is proposed to solve this ambiguity. Most of the techniques use the observed longitudinal magnetic field to calculate the configuration of the potential field. Then, the observed transversal magnetic field is directed along the potential transversal field. Calculations of electric currents imply deriving of the spatial derivative of the transversal magnetic field. In such a case, the magnitude, sign and spatial structure of electric currents and current helicity depend drastically on the correct 180-degree disambiguation of the transversal magnetic field. In the case of longitudinal magnetic field saturation inside a sunspot, the 180-degree disambiguation procedure directs the azimuthal component of the transversal magnetic field in the wrong direction resulting in incorrect estimation of electric currents and, consequently, of current helicity.

The saturation of the longitudinal magnetic field inside a sunspot can be eliminated by using additional information on spectral line. Thus, Su and Zhang [4] used 31 points of the spectral line profile to derive vector magnetic field by non-linear least squares fitting technique. A similar analysis was carried out by Bai et al. [5] who fitted six points of the Fe I 5324.18 Å spectral line profile by analytical Stokes profiles obtained in the Milne-Eddington atmosphere approximation.

In this paper, we make an attempt to improve the magnetic field measurements at a single point of the spectral profile at HSOS/SMFT by introducing non-linear relationship between the Stokes V/I and longitudinal magnetic field.

Methods

To establish the relationship between the Stokes V/I and B_z we performed the comparison of Stokes V/I acquired by HSOS/SMFT and longitudinal magnetic field measured by the Helioseismic and Magnetic Imager onboard the Solar Dynamics Observatory satellite (SDO/HMI) [6]. SDO/HMI is a full-disk filtergraph that measures the profile of photospheric Fe I 6173 Å line at six wavelength positions in two polarization states to derive the information on longitudinal magnetic field. The spatial resolution of the instrument is 1'' with 0.5''x0.5'' pixel size.

For comparison we used co-temporary magnetograms of randomly selected ten active regions observed between 2015 and 2018. Magnetograms acquired by SDO/HMI were rotated by the p -angle and rescaled to the pixel size of HSOS/SMFT of approximately 0.29''x0.29'' by a cross-correlation technique. Since SDO/HMI data are not affected by the atmospheric seeing, the magnetograms from the space-borne instrument were smoothed by a Gaussian kernel to imitate atmospheric distortion. Then, the same regions of the solar surface were cropped out from the HSOS/SMFT Stokes V/I maps and processed SDO/HMI magnetograms.

The HSOS/SMFT Stokes V/I versus SDO/HMI B_z distribution for all the magnetograms used in the comparison is shown in Figure 1. The red curve in the plot is the best least-square approximation of the distribution by a third order polynomial. One can see that the linear relationship holds for relatively weak magnetic fields while Stokes V/I starts to saturate for longitudinal magnetic field exceeding approximately 1000 G.

The essential key of our method is using two different calibration expressions for weak (B_{\parallel}^w) and strong (B_{\parallel}^s) longitudinal magnetic field. Indeed, for each value of measured Stokes V/I we can determine two corresponding values of B_{\parallel} at the calibration curve (see Figure 2). Based on the approximation of the distribution shown in Figure 1, we can write the following expression for deriving longitudinal magnetic field from Stokes V/I :

$$B_{\parallel}^w = 1.656 \cdot 10^4 (V/I) + 2.874 \cdot 10^6 (V/I)^3 \quad (2)$$

$$B_{\parallel}^s = \pm(1.983 \cdot 10^3 - 2.859 \cdot 10^5 (V/I)^2) \quad (3)$$

The next step is to figure out at which part of the calibration curve our particular pixel is, i.e. does this value of Stokes V/I in the pixel correspond to weak or strong magnetic field? To answer this question, we propose to employ the following. It is well known that the magnetic field in the photosphere suppresses the convection resulting in decreasing of plasma temperature and, as a consequence, of continuum intensity. Norton and Gilman [7] showed that a direct relationship exists between continuum intensity and the magnetic field strength. Hence, we can use readily obtainable Stokes I as a proxy of continuum intensity to figure out which part of the calibration curve must be used to derive the value of magnetic field from Stokes V/I : continuum intensity or Stokes I in the strong-magnetic-field regions is sufficiently lower than that in the weak-magnetic-field or quiet-Sun areas.

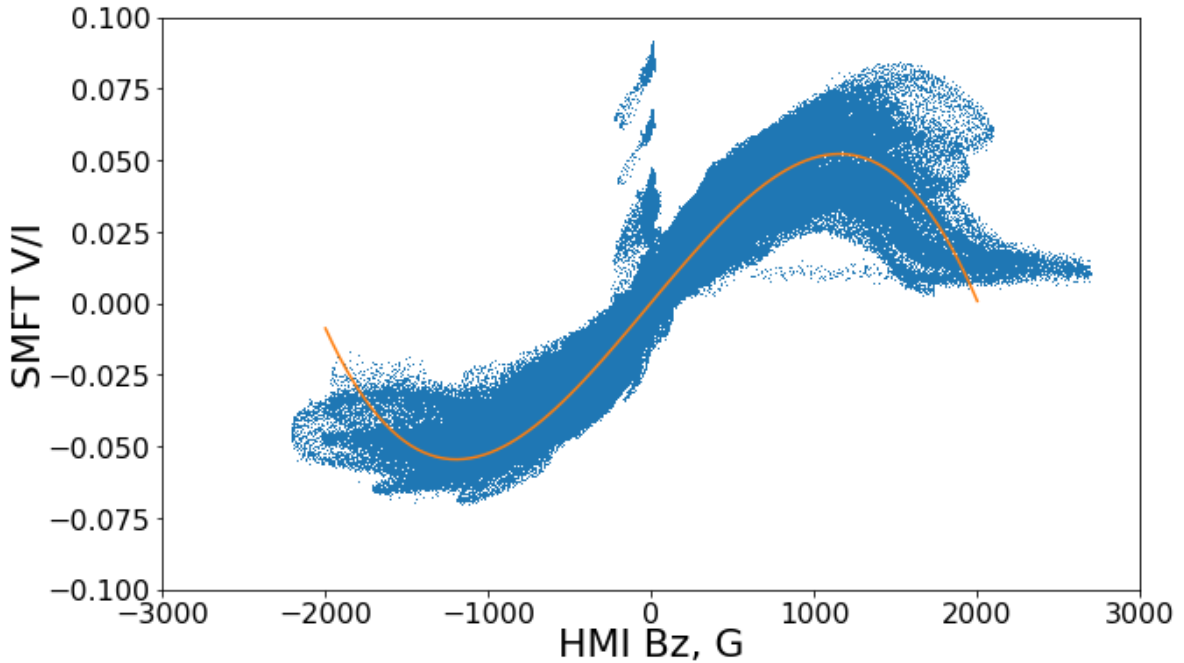


Fig. 1. SMFT Stokes V/I versus HMI B_z . The red curve shows the best third order polynomial approximation of the distribution.

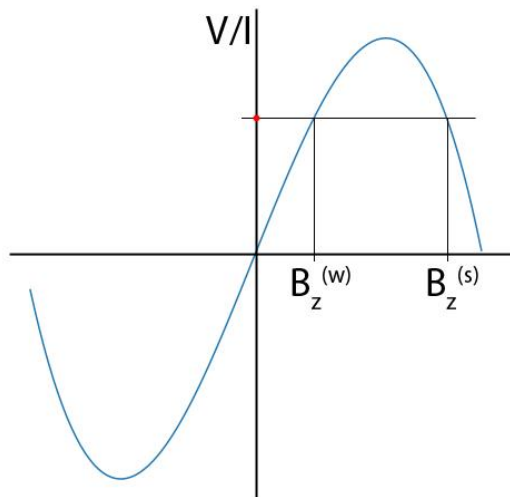


Fig. 2. Deriving longitudinal magnetic field from Stokes V/I value.

The obvious choosing of the threshold Stokes I_t value to separate pixels into two subsets of strong and weak magnetic field might be inappropriate: due to noise in the Stokes I maps two adjacent pixels with actually nearly the same value of magnetic field could be attributed to different parts of the calibration curve. As a result, sudden changes of B_{\parallel} might be observed in the derived map of the longitudinal magnetic field. We propose to set two thresholds, I_s and I_w , such that pixels with $I < I_s$ are definitely related to strong-field regions and pixels with $I > I_w$ are associated with quiet-Sun or weak-field regions.

If the required cadence of the data is not high enough manual choosing of the threshold values I_s and I_w by an observer is acceptable. One can use isolines of the continuum intensity to choose the thresholds such that pixels with $I < I_s$ are sunspot umbra pixels and pixels with $I > I_w$ are outer boundary of the penumbra and quiet-Sun pixels (Figure 3). Magnetic field in pixels with $I_s < I < I_w$ could be derived by, for example, interpolation methods.

All in all, the modified algorithm for deriving B_{\parallel} from Stokes V/I can be summarized as follows:

1. Separate all the pixels into two sets of strong and weak magnetic field pixels by applying thresholds I_s and I_w to Stokes I map. Pixels where $I_s < I < I_w$ could be omitted at this step.
2. Calculate longitudinal magnetic field in pixels using expressions (2) and (3) for strong and weak magnetic field pixels, respectively.
3. For each row or column of the magnetogram use (linear) interpolation to calculate magnetic field in pixels omitted at the first step.
4. Smooth the magnetogram to eliminate possible discontinuity at the boundaries of the interpolated segments.

The results of the algorithm applying to a sunspot slice of a magnetogram are shown in Figure 4. As one can see, the saturation in the sunspot umbra can be eliminated.

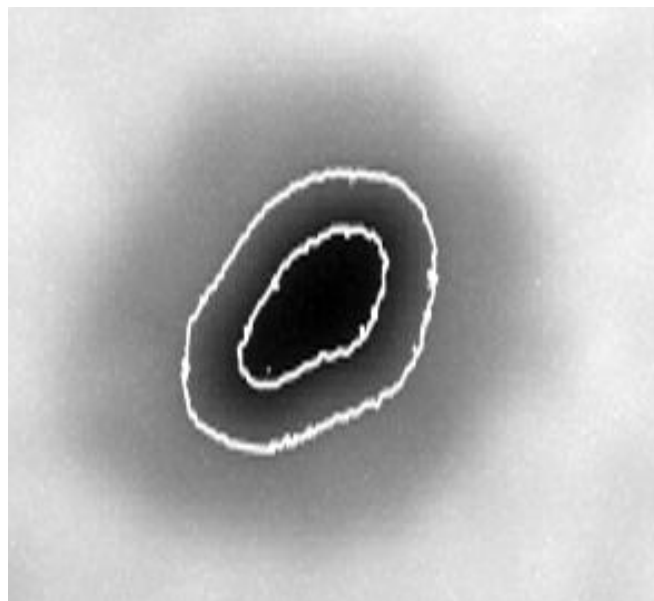


Fig. 3. An example of intensity isolines that could be used to set the intensity thresholds.

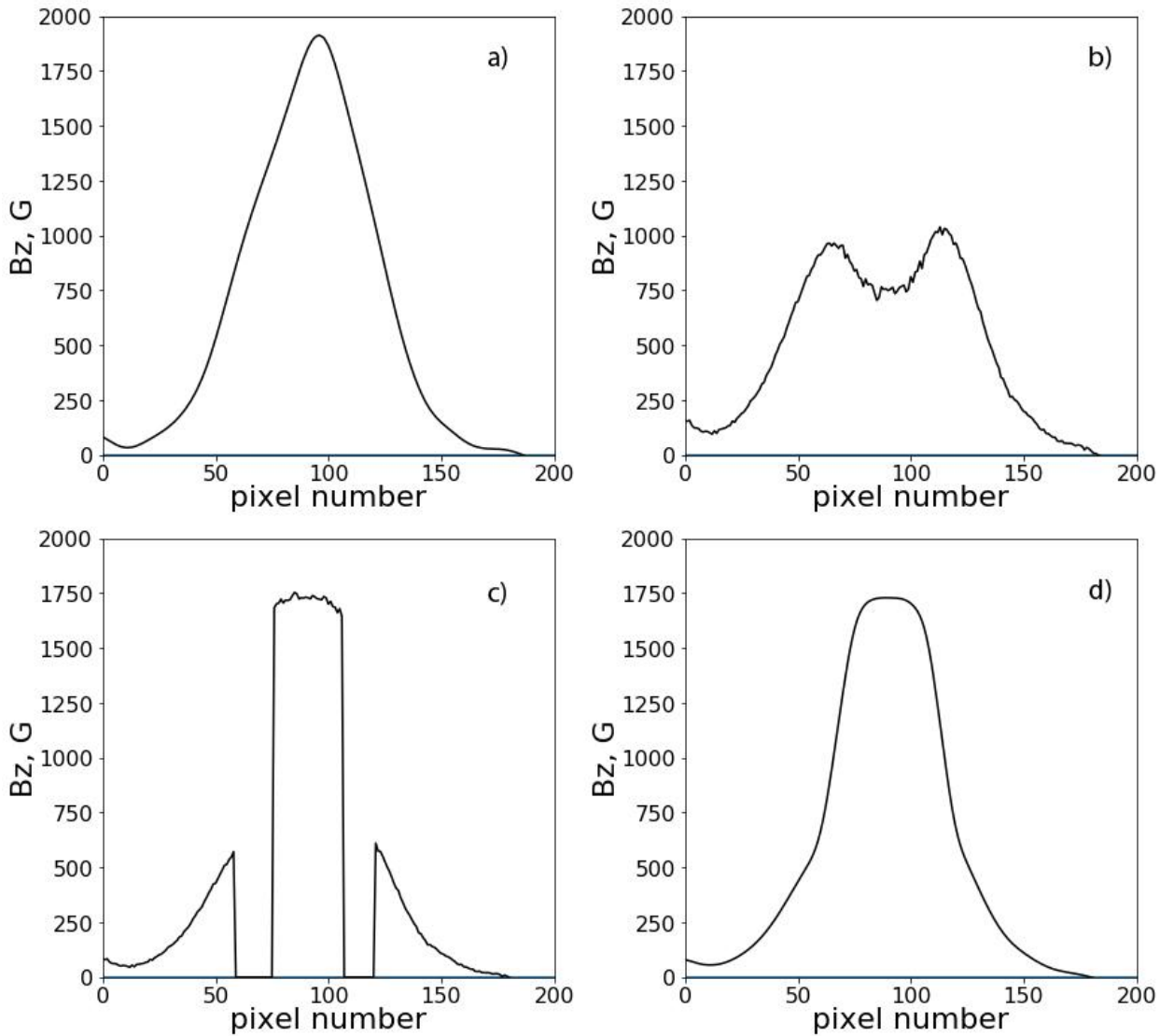


Fig. 4. The slice of a magnetogram: a) - magnetic field provided by SDO/HMI, b) – magnetic field derived from HSOS/SMFT Stokes V/I in the framework of the weak-field approximation, c) – magnetic field for strong and weak magnetic field regions derived from HSOS/SMFT Stokes V/I by equation (2) and (3), d) – magnetic field obtained by the proposed algorithm after interpolation and smoothing.

Results

To test the method, we derived longitudinal magnetic field of five active regions by linear weak-field approximation, equation 1, (Figure 5, middle column) and by the proposed algorithm (Figure 5, right column) from Stokes V/I acquired by HSOS/SMFT. Active regions' NOAA numbers and the dates of observations are in the titles of the panels. The SDO/HMI co-temporary magnetograms of the same active regions are shown in the left column of Figure 5 for comparison. The Stokes I thresholds were set to $I_s = 0.65I_c$ and $I_w = 0.4I_c$, where I_c is the Stokes I of the continuum intensity.

One can see the saturation in the magnetograms observed inside strong magnetic field concentration in the middle column of Figure 5 (indicated by red arrows). At the same, both SDO/HMI magnetograms and the magnetograms calculated by the proposed modified algorithms are free of this imperfection.

The SDO/HMI longitudinal magnetic field versus that derived from HSOS/SMFT data distribution for the selected magnetograms is shown in Figure 6. In contrast to Figure 1, quasi-linear relationship holds up to magnetic fields as high as 2500 G.

Conclusions

We proposed an algorithm aimed at deriving longitudinal magnetic field from Stokes V/I observed by HSOS/SMFT. The key feature of the algorithm is the non-linear relationship between magnetic field and Stokes V/I value.

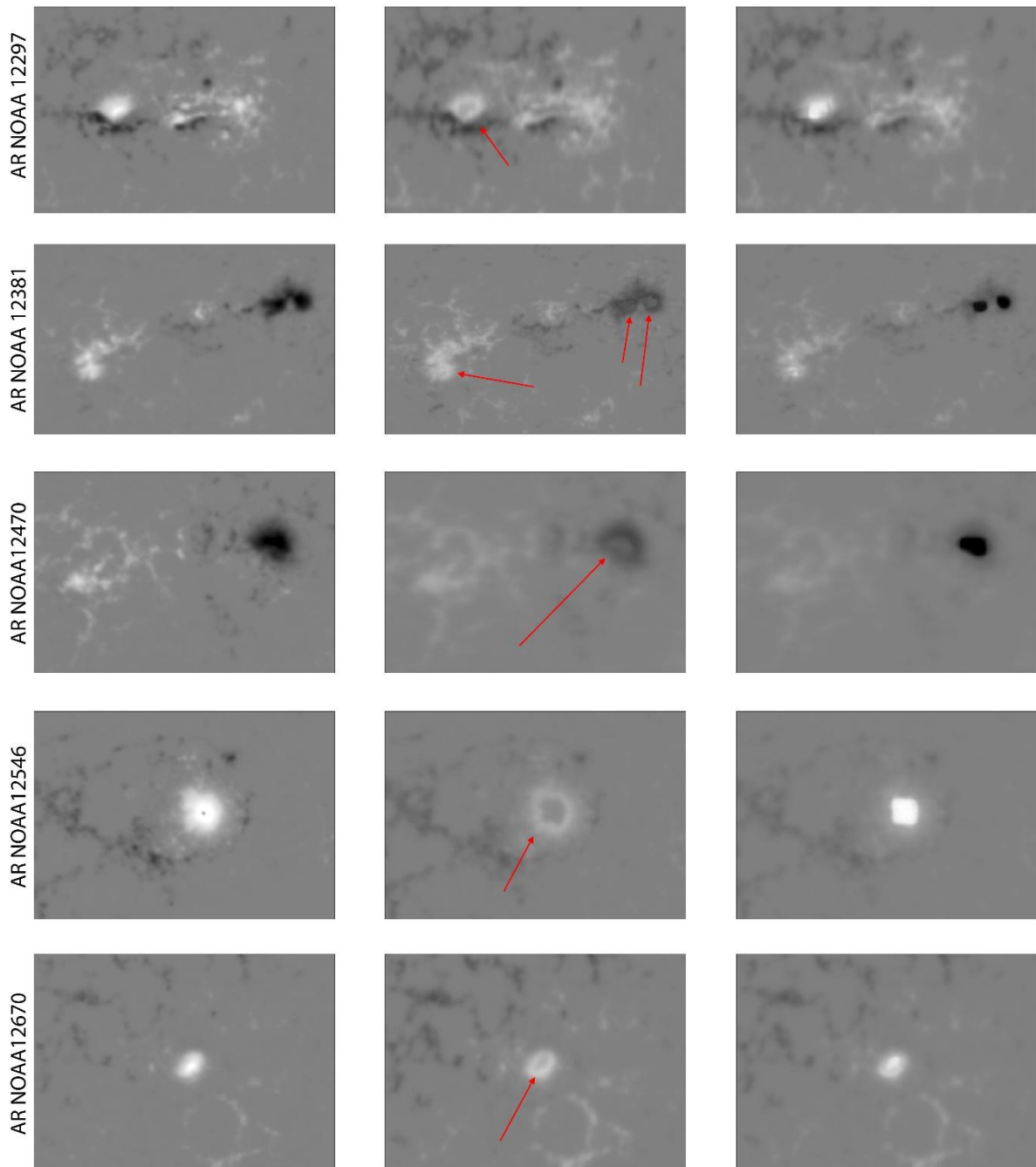


Fig. 5. Magnetograms for selected active regions: HMI (left column), SMFT (middle column), SMFT with the algorithm (right column). Red arrows points the saturation in SMFT observations.

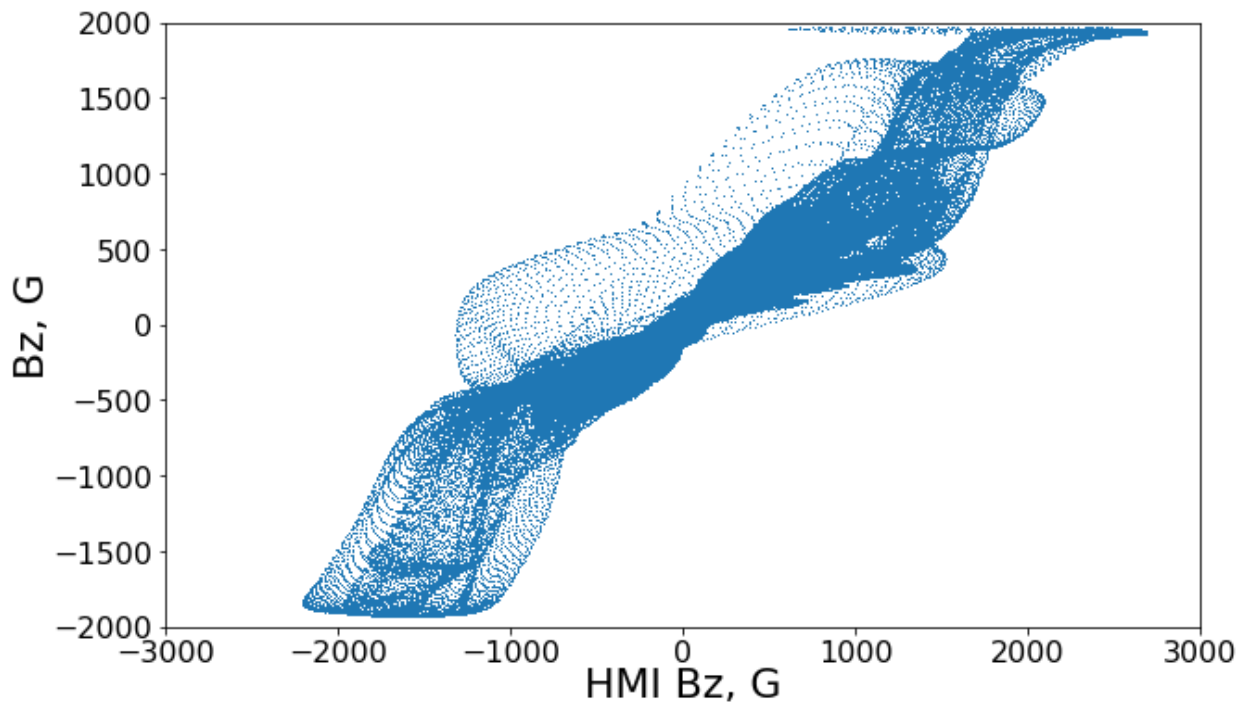


Fig 6. The SDO/HMI Bz versus modified HSOS/SMFT Bz for all the magnetograms shown in Figure 5.

References

- 1) Ai G.-X., 1987, Publ. Beijing Astron. Obs., 9, 27
- 2) Ai G.-X., 1982, Chin,Astron.Astrophys.5,129
- 3) Bai X. Y., Deng Y. Y., Su J. T., 2013, Sol. Phys., 282, 405
- 4) Su J.-T., Zhang H.-Q., 2004, Chin. J. Astron. Astrophys., 4, 365
- 5) Bai X.Y. et al, 2014, MNRAS, 445, 49
- 6) Scherrer P.H. et al, 2012, Sol. Phys., 275, 207
- 7) Norton A.A. and Gilman P.A., The Astrophys. J., 603:348–354, 2004